*Molecular Vision* 2016; 22:1361-1374 <http://www.molvis.org/molvis/v22/1361>
Received 9 June 2016 | Accepted 30 November 2016 | Published 2 December 2016



# PKR promotes choroidal neovascularization via upregulating the PI3K/Akt signaling pathway in VEGF expression

**Manhui Zhu,[1,4] Xiaojuan Liu,[2,4] Shengcun Wang,[3,4] Jin Miao,[3,4] Liucheng Wu,[3,4] Xiaowei Yang,[1,4] Ying Wang,[1,4] Lihua Kang,[1,4] Wendie Li,[1,4] Chen Cui,[1,4] Hui Chen,[1,4] Aimin Sang[1,4]**

**(The first two and last two authors contributed equally to this work.)**

*[1]Department of Ophthalmology, Affiliated Hospital of Nantong University, Nantong, Jiangsu, China; [2]Department of Pathogen Biology, Medical College, Nantong University, Nantong, Jiangsu, China; [3]Laboratory Animals Centre, Nantong University, Nantong, Jiangsu, China; [4]Jiangsu Province Key Laboratory for Inflammation and Molecular Drug Target, Medical College, Nantong University, Nantong, Jiangsu, PR China*

**Purpose:** The aim of this study was to investigate the functions of dsRNA-activated protein kinase (PKR) in choroidal neovascularization (CNV) and related signaling pathways in the production of vascular endothelial growth factor (VEGF).

**Methods:** A chemical hypoxia model of in vitro RF/6A cells, a rhesus choroid-retinal endothelial cell line, was established by adding cobalt chloride ($CoCl_2$) to the culture medium. PKR, phosphophosphatidylinositol 3-kinase (p-PI3K), phosphoprotein kinase B (p-Akt), and VEGF protein levels in RF/6A cells were detected with western blotting. PKR siRNA and the PI3K inhibitor LY294002 were used to evaluate the roles of the PKR and PI3K signaling pathways in VEGF expression with western blotting. In an ARPE-19 (RPE cell line) and RF/6A cell coculture system, proliferation, migration, and tube formation of RF/6A cells under hypoxic conditions were measured with 3-(4,5-dimethylthiazol-2-yl)-2,5-diphenyl tetrazolium bromide (MTT), Transwell, and Matrigel Transwell assays, respectively. In vivo CNV lesions were induced in C57BL/6J mice using laser photocoagulation. The mice were euthanized in a timely manner, and the eyecups were dissected from enucleated eyes. PKR, p-PI3K, p-Akt, and VEGF protein levels in tissues were detected with western blotting. To evaluate the leakage area, fundus fluorescein angiography and choroidal flat mount were performed on day 7 after intravitreal injection of an anti-PKR monoclonal antibody.

**Results:** The in vitro RF/6A cell chemical hypoxia model showed that PKR expression was upregulated in parallel with p-PI3K, p-Akt, and VEGF expression, peaking at 12 h. PKR siRNA downregulated PKR, p-PI3K, p-Akt, and VEGF expression. In addition, the PI3K inhibitor LY294002 greatly decreased the p-PI3K, p-Akt, and VEGF protein levels, but PKR expression was unaffected, indicating that Akt was a downstream molecule of PKR that upregulated VEGF expression. In the ARPE-19 (RPE cell line) and RF/6A cell coculture system, PKR siRNA reduced the migration and tube formation of the RF/6A cells. In vivo, PKR, p-PI3K, p-Akt, and VEGF expression increased and peaked at 7 days in the mouse CNV model induced by laser photocoagulation. Furthermore, on the RPE and choroid cryosections, PKR colocalized with CD31, suggesting that PKR was expressed by the vascular endothelium. The intravitreal injection of an anti-PKR monoclonal antibody decreased the progression and leakage area of CNV in mice.

**Conclusions:** PKR promotes CNV formation via the PI3K/Akt signaling pathway in VEGF expression. Additionally, the anti-PKR monoclonal antibody significantly decreased CNV in a mouse model, showing the antibody may have therapeutic potential in human CNV.

Age-related macular degeneration (AMD) is the leading cause of visual impairment and blindness in the elderly in industrialized nations [1,2]. There are two forms of AMD: One is neovascular (wet AMD), and the other is non-neovascular (dry AMD). Choroidal neovascularization (CNV) is a vital feature of wet AMD, which causes rapid progression to significant sight loss [3]. Currently, the standard treatment for CNV is antivascular endothelial growth factor (VEGF), which dramatically reduces blindness due to CNV [4]. However, patients require frequent intravitreal injections that lead to various complications, such as endophthalmitis [5] and RPE tears [6,7]. Therefore, further research on developing novel agents that target different molecules is needed to improve the antiangiogenic effects of CNV treatment.

Correspondence to: Hui Chen, Affiliated Hospital of Nantong University Eye Institute, 20 Xisi Road, Nantong, Jiangsu, 226001, China, Nantong, Jiangsu 226001, China; Phone: +86-13809082586; FAX: +86-513-85519820; email: chenhuieye@126.com

PKR, a dsRNA-activated serine-threonine protein kinase, whose autophosphorylation is induced by dsRNA, PKR-activating protein (PACT), and interferons, phosphorylates several target proteins [8]. PKR was previously considered to function primarily as a mediator of the antiviral response, but after extensive research, PKR is currently regarded to

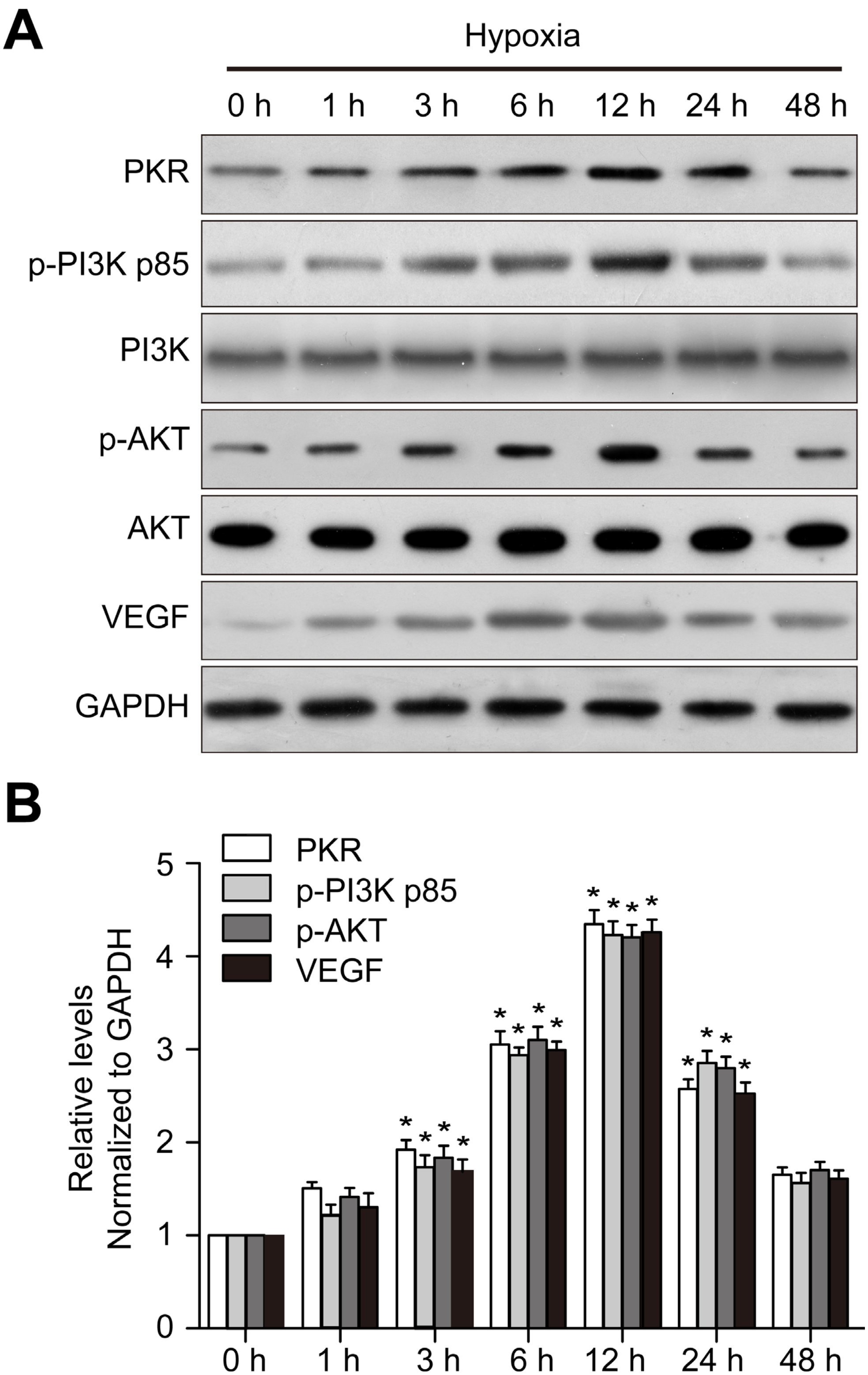


Figure 1. Chemical hypoxia induces PKR, p-PI3K, p-Akt, and VEGF expression in RF/6A cells in vitro. **A**: Western blot shows dsRNA-activated protein kinase (PKR), phosphophosphatidylinositol 3-kinase (p-PI3K), phosphoprotein kinase B (p-AKT), and vascular endothelial growth factor (VEGF) expression. **B**: The histogram shows the densitometric analysis of the average levels of PKR, p-PI3K, p-Akt, and VEGF to GAPDH. *$p<0.05$ compared with normal controls. n = 3 in each group.

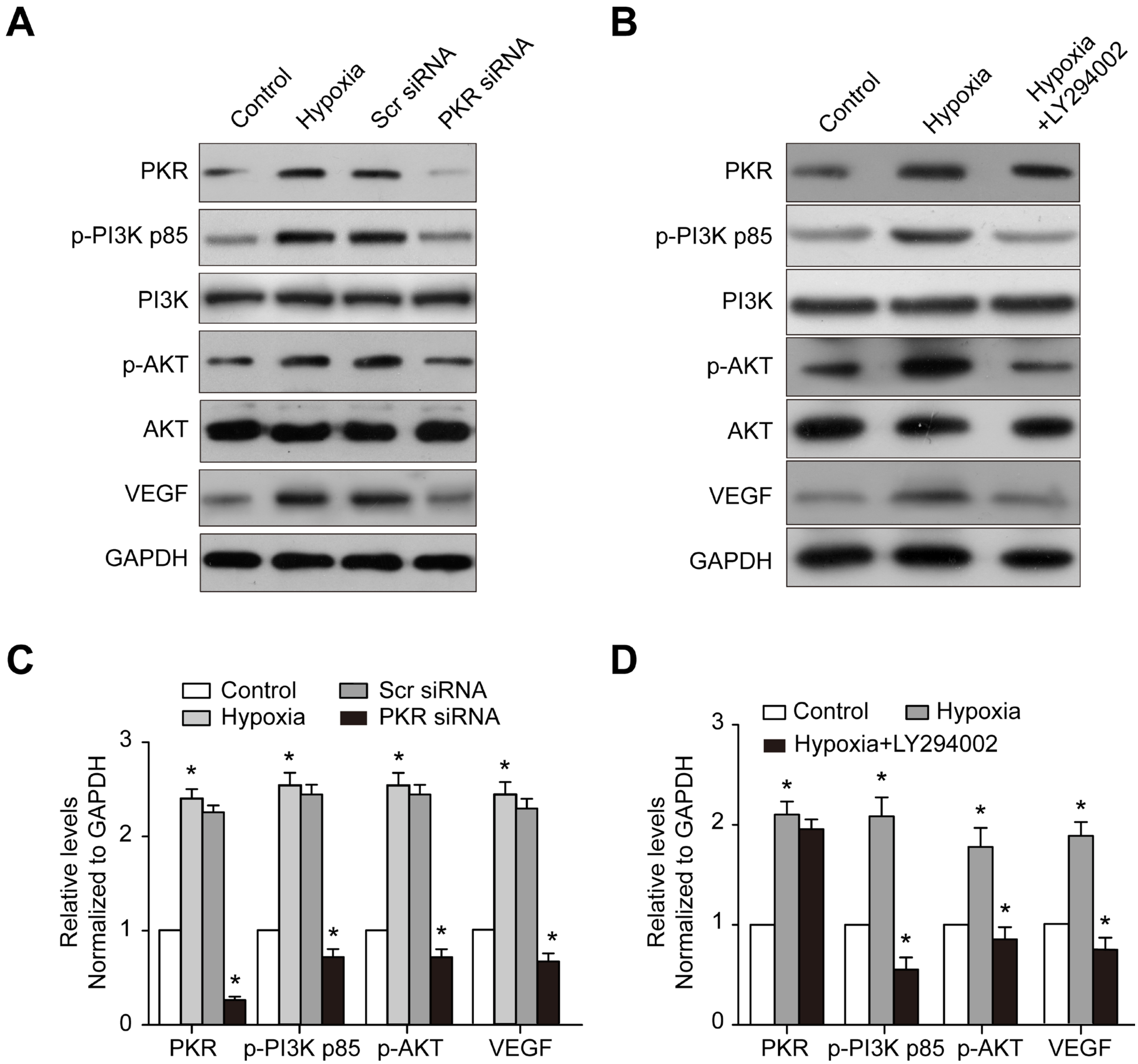


Figure 2. Effect of PKR siRNA and PI3K inhibitor LY294002 on hypoxia-induced PKR, p-PI3K, p-Akt, and VEGF expression in RF/6A cells. **A**: DsRNA-activated protein kinase (PKR), phosphophosphatidylinositol 3-kinase (p-PI3K), phosphoprotein kinase B (p-Akt), and vascular endothelial growth factor (VEGF) expression was detected with western blotting in the RF/6A cells following PKR siRNA transfection after 48 h. **C**: The histogram shows the densitometric analysis of the average levels for PKR, p-PI3K, p-Akt, and VEGF to GAPDH. Cells transfected with scramble siRNA were used as the negative control. **B**: The western blot shows PKR, p-PI3K, p-Akt, and VEGF expression in RF/6A cells treated with the PI3K inhibitor LY294002 for 30 min. **D**: The histogram shows the densitometric analysis of the average levels of PKR, p-PI3K, p-Akt, and VEGF to GAPDH. Hypoxic cells were used as the negative control. *$p<0.05$, statistically significantly different compared to the respective controls. Values represent means ± SD.

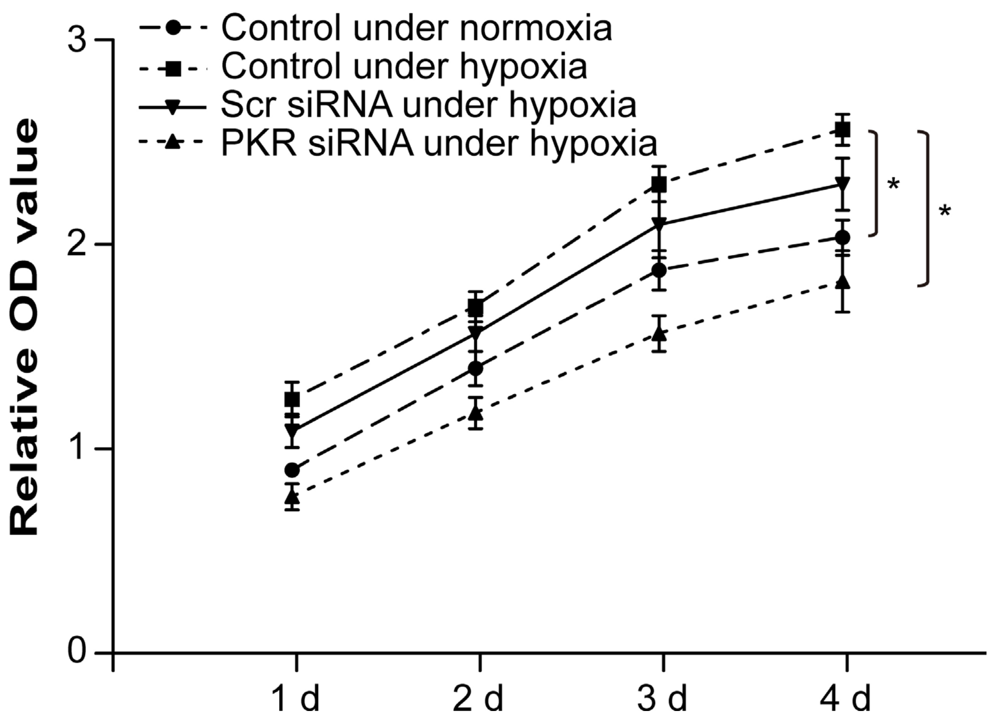


Figure 3. PKR promotes proliferation of RF/6A cells in a coculture system under hypoxic conditions. Detected with the cell counting kit 8 (CCK 8) assay, hypoxia increased RF/6A cell proliferation in the coculture system, whereas RF/6A cell proliferation was suppressed dramatically with dsRNA-activated protein kinase (PKR) silencing. *$p<0.05$, statistically significantly different compared to the respective controls. Values represent means ± SD.

be versatile. For instance, PKR is a novel player that functions to directly coordinate skeletal muscle differentiation via the phosphatidylinositol 3-kinase (PI3K)/protein kinase B (Akt) signaling pathway [9]. Furthermore, PKR can regulate proliferation of smooth muscle cells (SMCs) [10] and adherent molecule expression of endothelial cells (ECs) [11,12], indicating that PKR has a potential role in vascular system development. In addition, PKR was discovered to mediate angiogenesis via the VEGF pathway in peripheral artery disease [13]. Meanwhile, the PI3K/Akt signaling pathway is critical for ischemia and angiogenesis [14]. In human RPE (hRPE), the activation of Akt contributes to hypoxia-induced VEGF expression [15]. However, the involvement of PKR in CNV and related signaling pathways in the production of VEGF is unclear.

In the present study, we first detected the expression of PKR, p-PI3K, p-Akt, and VEGF in mouse CNV and RF/6A cell hypoxia models. We found that the expression levels of PKR, p-PI3K, p-Akt, and VEGF were upregulated. Second, we investigated the specific mechanism of PKR-mediated VEGF expression via PKR-specific siRNA and monoclonal antibodies. The results suggest that PKR may promote VEGF expression through the PI3K/Akt signaling pathway. Last, we investigated the role of PKR in CNV formation. We found intravitreal injection of anti-PKR monoclonal antibody alleviates CNV formation via inhibiting VEGF expression. These promising results suggest PKR may be a potential therapeutic target for human CNV treatment.

## METHODS

*Animals:* All experimental procedures were performed in accordance with the requirements of the Animal Welfare Committee of Nantong University. This study adhered to the ARVO Statement for the Use of Animals in Ophthalmic and Vision Research. The research protocol for the use of animals was approved by the Center for Laboratory Animals of Nantong University (Nantong, Jiangsu, China).

*Cell culture:* Human RPE cell line ARPE-19 was purchased from American Type Culture Collection (ATCC, Manassas, VA). A choroid-retinal endothelial cell line (RF/6A) from rhesus monkeys was obtained from the Cell Bank of the Chinese Academy of Sciences (Shanghai, China) and was identified as being of endothelial origin with cellular morphology, growth pattern, ultrastructure, immunocytochemistry, and immunodiffusion [16]. The cells were maintained in Roswell Park Memorial Institute (RPMI) 1640 medium supplemented with 10% fetal bovine serum (FBS; Gibco, Rockville, MD) and 100 U/ml penicillin-streptomycin mixtures (Gibco) at 37 °C in 5% $CO_2$. The culture medium was changed every 2 or 3 days. An in vitro RF/6A cell chemical hypoxia model was established by adding 200 µM cobalt chloride ($CoCl_2$) to the culture medium, and cells were

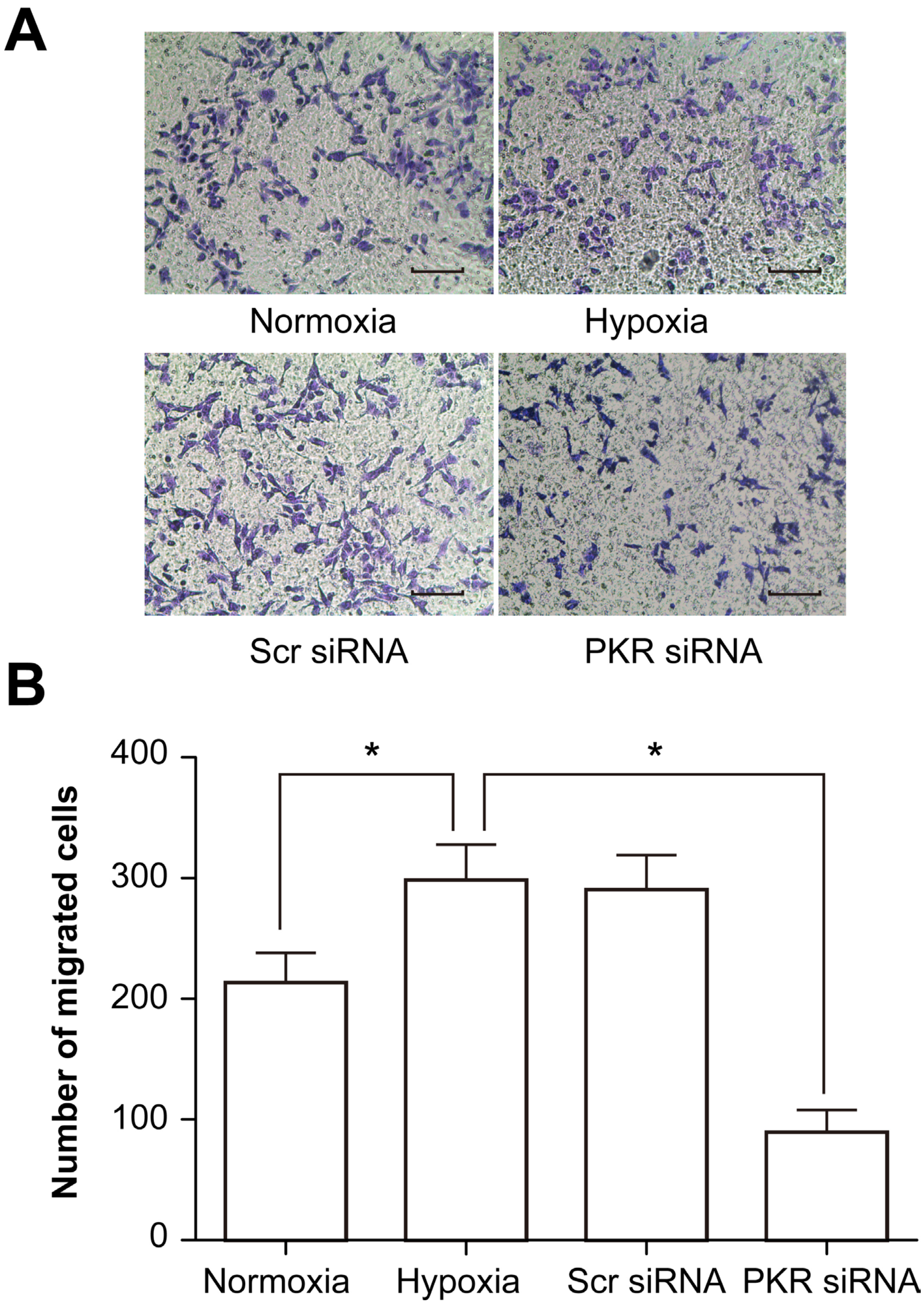


Figure 4. PKR promotes migration of RF/6A cells in a coculture system under hypoxic conditions. **A**: Crystal violet staining detected the migrated cells of each group: normal, hypoxic, scramble siRNA, and dsRNA-activated protein kinase (PKR) siRNA. Representative photographs of migrated RF/6A cells (200× magnification). **B**: The average number of migrated RF/6A cells per field. *p<0.01, PKR siRNA group versus the hypoxic group. Values represent means ± SD.

harvested after 1, 3, 6, 12, 24, and 48 h. Cells without $CoCl_2$ treatment were regarded as the normal control.

*PKR gene silencing:* A total of 1 × $10^6$ RF/6A cells per well were seeded in six-well plates and allowed to grow overnight. Transfection of PKR siRNA (5′-GGA TTC GGG TTA CTT GTA A-3′, RiboBio, Guangzhou, China) was performed using Lipofectamine 2000 (Invitrogen, Carlsbad, CA) following the manufacturer's protocol. Briefly, for the six-well plates, 4 µg DNA was mixed with 10 µl Lipofectamine 2000 at a final concentration of 2 µg DNA/ml and dissolved in RPMI 1640 without serum. The resulting complex was incubated at room temperature for 20 min to generate a transfection mixture that was then added to the cells, which were incubated for 4 to 6 h. Next, the cells were washed with RPMI 1640 and incubated

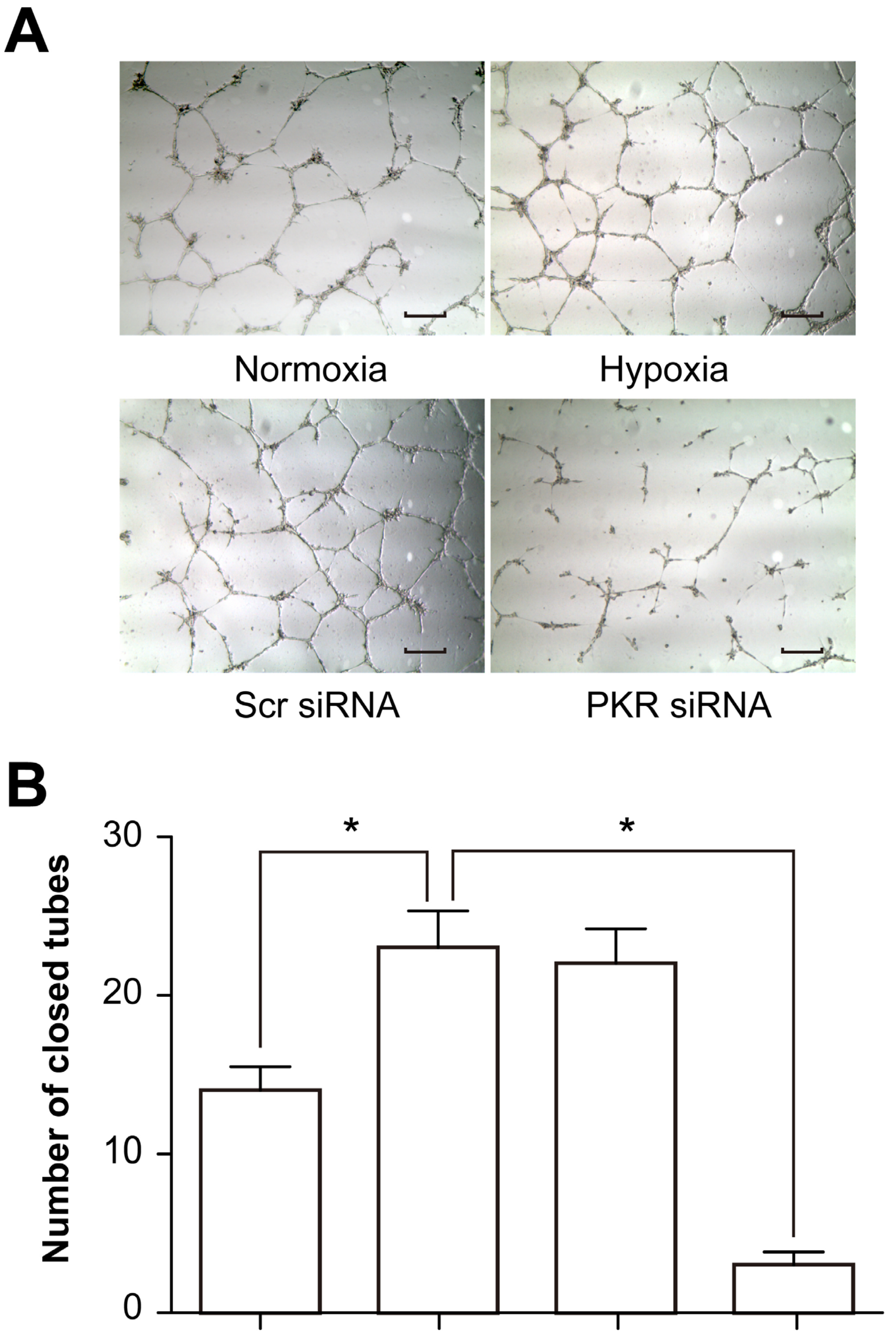


Figure 5. PKR promotes tube formation of RF/6A cells in a coculture system under hypoxic conditions. **A**: Microscopic images showing tube formation in each group: normal, hypoxic, scramble siRNA, and dsRNA-activated protein kinase (PKR) siRNA. Representative photographs of tube formation of RF/6A cells (200× magnification). **B**: Decreased tube formation was observed when the cocultured RF/6A cells were transfected with PKR siRNA under hypoxia. *p<0.01, PKR siRNA group versus the hypoxia group. Values represent means ± SD.

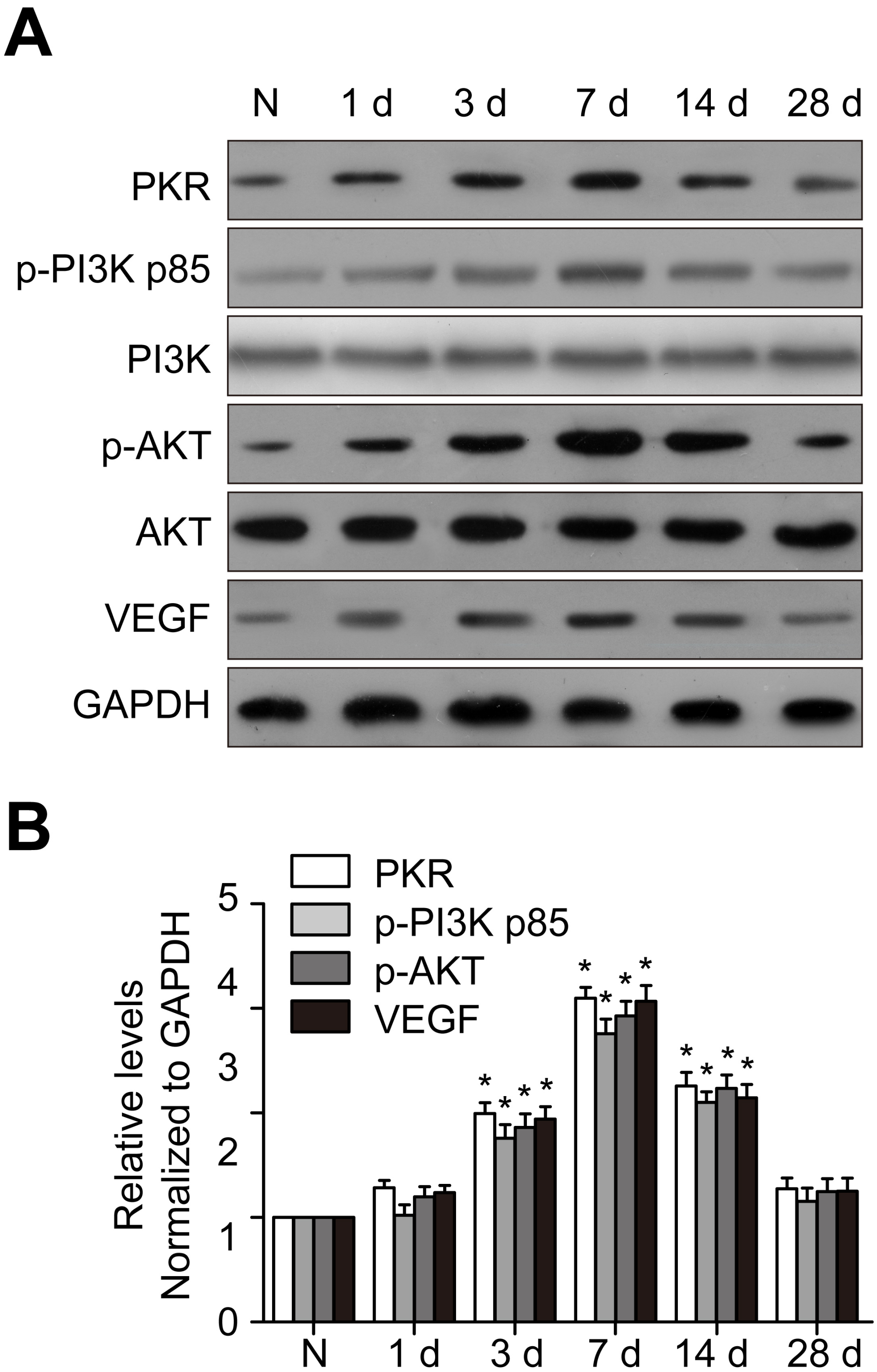


Figure 6. PKR, p-PI3K, p-Akt, and VEGF expression is upregulated in a mouse CNV model. The mouse choroidal neovascularization (CNV) model was created with laser photocoagulation. **A**: DsRNA-activated protein kinase (PKR), phosphophosphatidylinositol 3-kinase (p-PI3K), phosphoprotein kinase B (p-Akt), and vascular endothelial growth factor (VEGF) protein levels were detected with western blotting. GAPDH was used as the loading control. **B**: The histogram shows the densitometric analysis of the average levels of PKR, p-PI3K, p-Akt, and VEGF to GAPDH. *p<0.05, statistically significantly different from the normal control. Values represent means ± SD.

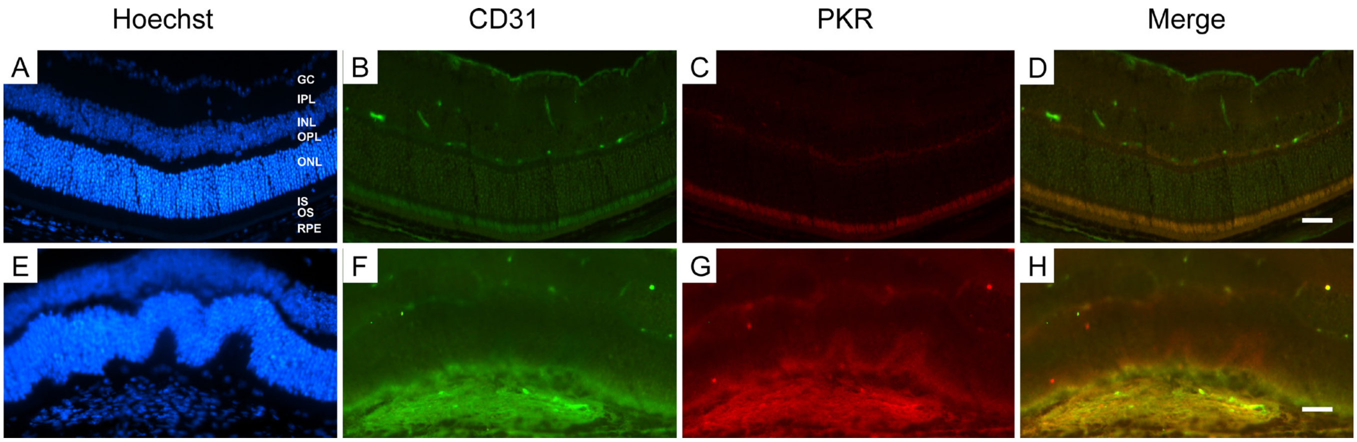


Figure 7. PKR is localized in endothelial cells. Cellular localization of dsRNA-activated protein kinase (PKR) in the retina and choroid cryosections was determined with double immunostaining together with endothelial marker CD31. Scale bar = 50 µm.

in RPMI 1640 with 10% FBS for an additional 48 h. Then, the cells were collected for western blot analysis.

*In vitro cell proliferation assay:* To test the effects of RPE cells on RF/6A cell proliferation under hypoxic conditions, a proliferation assay model was used. The RF/6A cells were plated at a density of 1 × $10^5$ cells/$cm^2$ in 24-well plates in complete medium and allowed to adhere overnight. Next, cells were transfected with PKR siRNA and scramble siRNA before 0.4 µm pore-size inserts were placed in the wells. Medium containing 200 µM $CoCl_2$ was added and was changed every 2 days. At the end of each time point, 20 µl of 5 mg/ml 3-(4,5-dimethylthiazol-2-yl)-2,5-diphenyl tetrazolium bromide (MTT; Sigma, St. Louis, MO) was added to each well for 4 h, then the supernatant was discarded, and 150 µl dimethyl sulfoxide (DMSO) was administered for 10–15 min. The absorbance was recorded at 570 nm with a Microplate Reader (Model 680, Bio-Rad, Hercules, CA). Each experimental condition was tested at least in triplicate.

*In vitro cell migration assay:* To test the effect of RPE cells on RF/6A cell migration under hypoxic conditions, a migration assay model was used. The RPE cells were plated at a density of 1 × $10^5$ cells/$cm^2$ in 24-well plates with medium containing 200 µM $CoCl_2$ added to the wells for 12 h. The RF/6A cell migration assay was performed using Matrigel-coated, Costar Transwell inserts with 8.0 mm pore size. Briefly, 5 × $10^4$ RF/6A cells were seeded on the inserts and incubated with RPMI 1640 containing 1% FBS. After 1 h for attachment, the inserts were transferred to 24-well plates as described above. After incubation for 4 h, the inserts were fixed with 4% paraformaldehyde, stained with 0.1% crystal violet for 30 min, and photographed under a light microscope (Olympus, Tokyo, Japan). Five random fields (× 200) were chosen in each insert, and the cell number was quantified manually.

*In vitro tube formation assay:* ARPE-19 cells were plated in the Transwells with 8 µm pore size inserts, which were put in the wells where the RF/6A cells had been plated. Briefly, Matrigel was thawed and laid in 24-well culture plates for a total volume of 200 µl in each well. The plates were stored at 37 °C for 30 min to form a gel layer. After gel polymerization, 2 × $10^4$ RF/6A cells were seeded in each well and incubated with RPMI 1640 supplemented with 0.5% FBS for 24 h at 37 °C in humidified air with 5% $CO_2$. The closed networks of tubes in each well were observed with an inverted phase-contrast microscope (Olympus, Tokyo, Japan). Incomplete networks were excluded. The experiments were performed in triplicate, and five fields from each chamber were counted and averaged.

*Laser-induced mouse CNV:* Adult C57BL/6J (B6) mice were anesthetized by intraperitoneal injection with 45 mg/kg pentobarbital sodium, and the pupils were dilated with topical administration of tropic amide phenylephrine eye drops (Santen, Osaka, Japan). Four burns were made with laser photocoagulation (647.1 nm; 50 mm spot size; 0.05 s duration; 200 mW) in each retina with a hand-held contact fundus lens (Ocular Instruments, Bellevue, WA) in the 3, 6, 9, and 12 o'clock positions between retinal vessels in the peripapillary area of both eyes. Only the burns that produced a bubble, indicating the rupture of Bruch's membrane, were counted in the study. All mice were randomly divided into five groups based on the time following laser treatment (normal, 1 day and 3, 7, 14, and 28 days). For western blot analysis, each group included 24 mice with laser treatment and 15 control mice without laser treatment. In the control and post-laser 7 day groups, another 45 mice (90 eyeballs) from each group were used for choroidal flat mount and immunofluorescence staining.

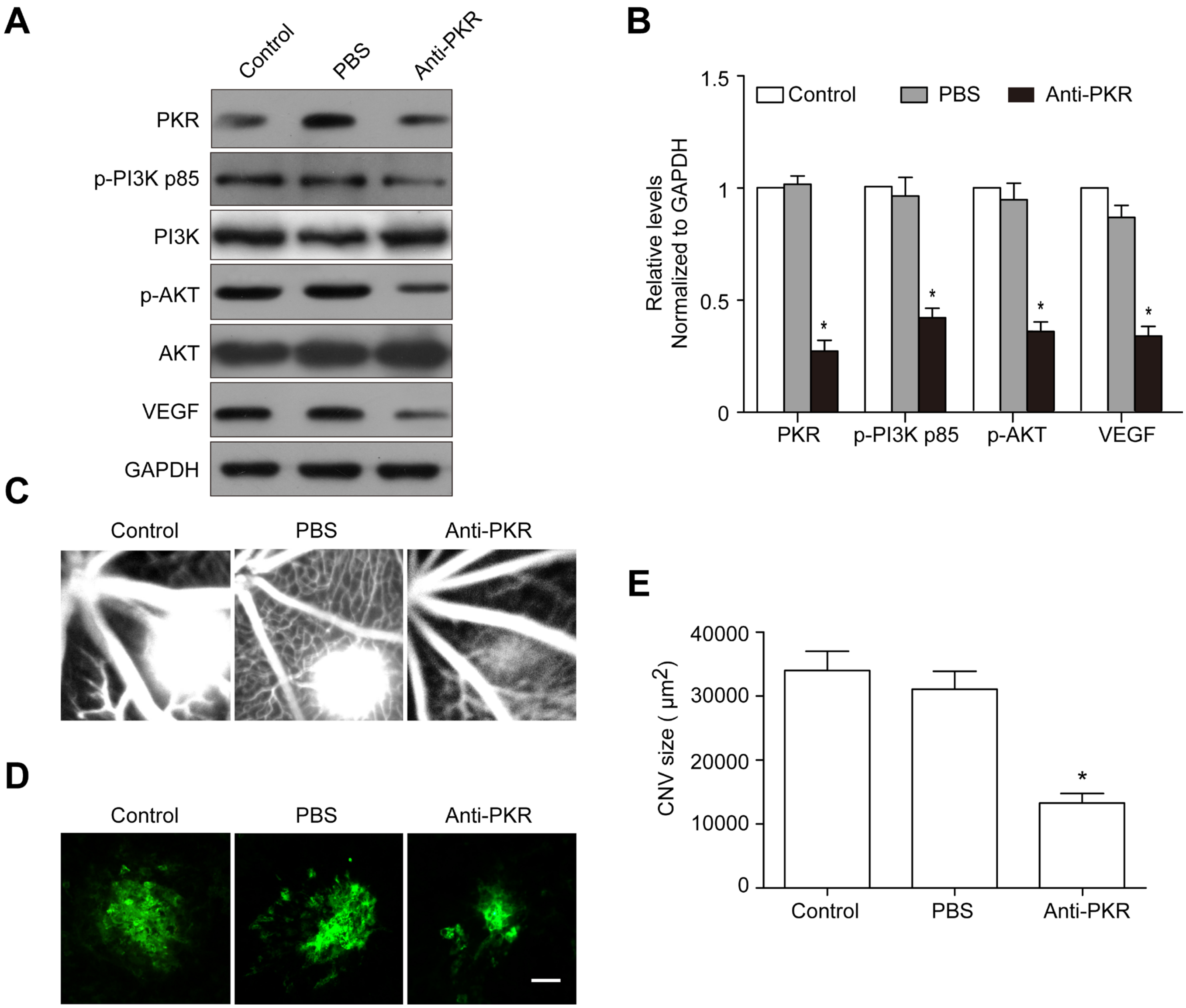


Figure 8. PKR monoclonal antibody intravitreal injection attenuates CNV. **A**: Western blot analysis showed that dsRNA-activated protein kinase (PKR), phosphophosphatidylinositol 3-kinase (p-PI3K), phosphoprotein kinase B (p-Akt), and vascular endothelial growth factor (VEGF) expression in the choroid-RPE-retina complex at day 7 after laser coagulation. **B**: Quantification graphs for PKR, p-PI3K, p-Akt, and VEGF to GAPDH. *p<0.01, anti-PKR versus PBS. **C**: Hyper-fluorescent leakage surrounding the laser spots was weak in the anti-PKR injection mice retinas. **D**: Representative images of isolectin B4 staining of the RPE-choroid-sclera whole mount from the control and PKR antibody injection groups 7 days after laser photocoagulation. **E**: Quantitative measurement of the choroidal neovascularization (CNV) area. *p<0.01, anti-PKR versus PBS.

*Western blot:* To detect the protein levels of the molecules, we extracted the mouse choroid-RPE-retina complex from three mice at 1 day and 3, 7, 14, and 28 days after the laser injury and used in vitro cell lysates. The proteins and a molecular weight marker were separated by 10% sodium dodecyl sulfate–polyacrylamide gel electrophoresis (SDS–PAGE) and transferred to a polyvinylidene difluoride (PVDF) membrane. The membrane was then incubated with primary antibodies for PKR (1:500; Santa Cruz Biotechnology, Santa Cruz, CA), p-PKR (1:500; Santa Cruz Biotechnology), p-PI3K (1:500; Cell Signaling Technology, Danvers, MA), PI3K (1:500; Cell Signaling Technology), VEGF (1:500; Santa Cruz Biotechnology), Akt (1:500; Cell Signaling Technology), and p-Akt (1:500; Cell Signaling Technology). The antibodies were incubated in 5% skim milk overnight at 4 °C and reacted with horseradish peroxidase (HRP)-conjugated secondary antibodies (1:2,000; Thermo Scientific, Rockford, IL) at 37 °C for 2 h. Extensive washes in 0.05% Tween-20 in Tris-buffered saline (TBS) were followed by incubation with anti-GAPDH (1:1,000; Sigma-Aldrich, Saint Louis, MO). The blots were then incubated with the chemofluorescent reagent enhanced chemiluminescence (ECL; Thermo Scientific, Rockford, IL) and exposed to X-ray film in the dark. The intensity of the GAPDH signal was used as an endogenous control, and the band optical density was quantified using Image J (National Institutes of Health, Bethesda, MD).

*Immunofluorescence:* PKR tissue localization was examined on 8 µm cryosections (on day 7 after laser photocoagulation). The cryosections were blocked with 1% bovine serum albumin (BSA) for 4 h at room temperature and then incubated with antibodies for PKR (1:50; Santa Cruz Biotechnology) and CD31 (1:50, Abcam, Cambridge, MA) at 4 °C overnight. For CD31 staining, antigen retrieval was performed by incubating the sections in a heated water bath at 37 °C for 10 min. Thereafter, the slides were stained with Alexa Fluor 488 conjugated goat anti-mouse immunoglobulin G, Alexa Fluor 546 conjugated goat anti-rabbit IgG (1:200; Invitrogen), and Hoechst (1:2,000; Sigma-Aldrich). The photomicrographs were obtained using a digital high-sensitivity camera (Hamamatsu, ORCA-ER C4742–95; Hamamatsu, Japan).

*Intravitreal injection:* The intravitreal injection of 1 µl of anti-PKR monoclonal antibody (200 ng/ml) or vehicle (PBS solution; 135 mM NaCl, 2.7 Mm KCl, 1.5 mM $KH_2PO_4$ , and 8 mM $K_2HPO_4$, pH 7.2) was administered on day 1, and mice were killed on day 7 after laser treatment. The control group represented laser-induced CNV without any injection.

*Choroidal flat mount:* On day 7, after laser coagulation, 30 eyes (six eyes from three mice/each group) were subjected to choroidal flat mounts. The eyes were enucleated and immediately fixed in 4% paraformaldehyde (Guoyao Group of Chemical Reagents, Beijing, China) in pH 7.3 PBS for 1 h. Under a biopsy microscope, the anterior segments were wiped out, and the neurosensory retinas were detached and separated from the optic nerve head. The remaining eyecups were washed with cold immunocytochemistry buffer (0.5% BSA, 0.2% Tween-20, and 0.1% Triton X-100) in PBS. A 1 mg/ml solution of Alexa Fluor 568 conjugated isolectin-B4 (1:100) was prepared in immunocytochemistry buffer. The eyecups were incubated with the fluorescent dyes in a humidified chamber at 4 °C with gentle shaking for 4 h, followed by washing with cold immunocytochemistry buffer. Four or five radial cuts were made toward the optic nerve head for flat mounting the sclera-choroid-RPE complexes together with the gel (Gel-mount; Biomedia Corp., Foster City, CA). The samples were covered and sealed for microscopic analysis.

*Fundus fluorescein angiography:* To confirm the inhibitory effect of the anti-PKR monoclonal antibody on CNV formation, fluorescein angiography was performed on day 7 after laser photocoagulation. The development of CNV was evaluated using a digital fundus camera connected to a slit-lamp delivery system (Kanghua, Chongqing, China), which was captured 4 min after 0.3 ml of 2% fluorescein sodium (Alcon Laboratories, Irvine, CA) was injected into the intraperitoneal cavity of mice as previously described [17].

*Statistical analysis:* All values were presented as the mean ± standard deviation (SD). One-way ANOVAs were used for statistical comparisons of multiple groups. Descriptive statistics were performed using Stata statistical software version 11.0 (Stata Corp, College Station, TX). A p value of less than 0.05 was considered statistically significant. Each experiment consisted of at least three replicates.

## RESULTS

*PKR, p-PI3K, p-Akt, and VEGF expression increases in RF/6A cells under hypoxic conditions:* To explore the function of PKR in CNV, we examined PKR, p-Akt, and VEGF expression in RF/6A cells after $CoCl_2$ treatment. As expected, western blotting showed that PKR, p-PI3K, p-Akt, and VEGF expression was upregulated in a similar time-dependent manner under hypoxic conditions (Figure 1), suggesting that PKR may be associated with VEGF expression.

*PKR siRNA and Akt-specific inhibitor downregulated VEGF expression:* To test whether PKR regulates VEGF expression via the Akt signaling pathway in RF/6A cells under hypoxic conditions, PKR expression in RF/6A cells was knocked down by PKR siRNA transfection, and the p-Akt and VEGF protein levels were evaluated with western blotting. PKR siRNA downregulated the PKR protein level by 88 ± 8% in the RF/6A cells (Figure 2A,C). Accordingly, the p-PI3K, p-Akt, and VEGF protein levels were downregulated by 65 ± 3% and 78 ± 5%, respectively, in the RF/6A cells in the PKR siRNA group compared to the control group (Figure 2A,C). We further investigated whether the PI3K/Akt signaling pathways were involved in PKR regulating VEGF expression in CNV, demonstrating that the PI3K inhibitor LY294002 greatly decreased the p-PI3K, p-Akt, and VEGF protein levels. However, PKR expression was unchanged, indicating that Akt was a downstream molecule of PKR and associated with VEGF expression.

*Promotion of RF/6A cell proliferation by PKR in a coculture system under hypoxic conditions:* An RPE-RF/6A coculture system was used to investigate the precise effects of PKR on the proliferation of RF/6A cells when induced by ARPE-19 cells under chemical hypoxic conditions. The MTT assay showed that PKR overexpression in RF/6A cells significantly increased cell proliferation under hypoxic conditions in the coculture system compared to the normoxia group. In contrast, cell proliferation was suppressed by silencing PKR expression in the hypoxic RF/6A cells using PKR siRNA transfection (Figure 3).

*Promotion migration of RF/6A cells by PKR in a coculture system under hypoxic conditions:* The effects of PKR on the migration of RF/6A cells in a coculture system under hypoxic conditions were also investigated. The number of RF/6A cells that migrated across the insert in the hypoxia group increased by 32.6% compared with the control normoxia group, whereas the RPE- and hypoxia-induced RF/6A cell migration decreased remarkably by 58.6% in PKR siRNA-transfected RF/6A cells compared with the hypoxia group (Figure 4).

*Promotion of tube formation of RF/6A cells by PKR in a coculture system under hypoxic conditions:* Tube formation is a very important function of ECs. RF/6A cells grown in a collagen matrix gel under hypoxic conditions showed enhanced tube formation. These results were in agreement with the proliferation assay (MTT assay) because the ability of ECs to form tube-like structures is partly related to cell proliferation. When PKR expression was inhibited, tube formation was reduced significantly compared with the hypoxia group (Figure 5).

*PKR, p-PI3K, p-Akt, and VEGF expression increased in the mouse CNV model:* To identify PKR, p-PI3K, p-Akt, and VEGF expression in a mouse CNV model, we extracted protein from the choroid-RPE-retina complex for western blot analysis. After laser injury, PKR expression was upregulated and peaked at 7 days, showing a similar time-dependent trend with p-Akt and VEGF (Figure 6). To identify the cellular localization of PKR inside the CNV site, we performed double immunostaining of PKR with CD31, a marker for endothelial cells, showing that inside the CNV site, PKR was localized in the vascular endothelium (Figure 7).

*The anti-PKR monoclonal antibody suppresses PKR, p-PI3K, p-Akt, and VEGF expression and alleviates the leakage area of CNV:* We next explored PKR, p-PI3K, p-Akt, and VEGF expression following the anti-PKR monoclonal antibody intravitreal injection in a mouse CNV model. The PKR protein levels in the choroid-RPE-retina complex were reduced dramatically in the anti-PKR injection group compared with the control and PBS injection groups. Furthermore, p-PI3K, p-Akt, and VEGF expression showed a similar decreasing tendency as PKR following anti-PKR injection (Figure 8A,B). The fluorescein angiogram assay showed that the leakage area of CNV was smaller in the anti-PKR injection group than in the PBS injection group on day 7 after laser photocoagulation (Figure 8C). The choroidal flat mount showed that the area of CNV was smaller, and there were fewer vessel tubes in the anti-PKR injection group compared with the PBS injection group (Figure 8D,E).

## DISCUSSION

AMD is the leading cause of blindness in the elderly in Western nations [18]. Thus, experimental animal models of CNV have become essential to elucidate the complicated cellular and molecular mechanisms underlying AMD pathogenesis, as well as filtering tools for new drugs [19]. The robust and easily accessible laser-induced mouse CNV model is the most widely accepted and commonly used model of neovascular AMD (nAMD) [20], becoming a universally used model of angiogenesis in recent years [21]. As part of our experimental design, laser-induced CNV was followed at regular time intervals (days 0, 1, 3, 7, 14, and 28) to evaluate VEGF expression during mouse CNV lesion progression. The data for the VEGF protein levels suggested that CNV peaked 7 days following laser treatment, which is in agreement with previous research [22,23].

Although there is still uncertainty about the exact pathogenesis of wet AMD, many involved mechanisms are already partially known and may be promising targets for therapy. Currently, VEGF represents the most important molecular target in the treatment of nAMD [24]. Current treatment strategies for nAMD place a significant treatment burden on patients and oculists. In the current era of individualized treatment strategies, most oculists practice either an as-needed (PRN) dosing regimen or treat-and-extend approach. Both strategies require a considerable number of office visits and injections [25]. Because many patients with AMD are older, they often need a caregiver to bring them for their appointments. Finally, current anti-VEGF strategies include frequent visits and injections ad infinitum for many patients. Therefore, searching for the molecules and underlying mechanisms that regulate VEGF expression and function id extremely urgent for the development of nAMD therapeutic strategies. In this study, we found that PKR promotes CNV via upregulating the PI3K/Akt/VEGF signaling pathway, identifying a novel VEGF up-stream regulator.

PKR, an interferon-inducible dsRNA-dependent protein kinase, exerts multiple cell effects such as antiviral, antitumor, and immunomodulatory effects [26-28]. Although the main direct PKR activator is dsRNA (produced during infection of several viruses and detected at low doses in mammalian cells), PKR is also activated by multiple cellular stresses, including cytokines, calcium stress, oxidative stress, endoplasmic reticulum stress, lipo stress, and amyloid-β

(Aβ) peptide accumulation [29,30], or through PACT [31,32]. A previous study revealed that PKR expression was markedly upregulated in human umbilical vein endothelial cells (HUVECs) and was indispensable for endothelial cell proliferation, migration, and tube formation. In vitro and in vivo studies suggest that PKR plays a key role in angiogenesis through the VEGF pathway [13]. However, soluble VEGF cannot increase the proliferation of solo CECs, and coculture conditioned media enhance CEC proliferation, indicating that growth factors other than VEGF promote CEC proliferation [33]. In our study, we also found that PKR expression was upregulated in the $CoCl_2$-treated RF/6A cell hypoxia model and the laser-induced CNV mouse model. Inhibition of PKR suppresses the proliferation and migration of RF/6A cells, as well as VEGF expression. Intravitreal injection of the PKR antibody relieves the progression of CNV in laser-exposed mice.

PKR is also reportedly involved in the activation of the NOD-like receptor (NLR) family, Pyrin domain containing 1 (NLRP1), Pyrin domain containing 3 (NLRP3), CARD domain containing 4 (NLRC4), and absent in melanoma 2 (AIM2) inflammasomes [34]. Inflammasomes are multiprotein complexes that detect and respond to foreign and endogenous danger signals by activating caspase-1. Active caspase-1, in sequence, matures proinflammatory interleukin-1beta (IL-1β) and IL-18 by cleaving their proforms to biologically active cytokines. A recent study showed that in rodents, intravitreal or systemic inoculation of murine IL-18 (SB-528775) can prevent experimentally induced CNV [35]. The receptor components in the best-known inflammasomes in the NLR family are usually NLRP1, NLRP3, or NLRC4 [36]. Currently, the NLRP3 inflammasome is the most thoroughly studied, and the active NLRP3 inflammasome is revealed to be present in human RPE cells [37,38]. One of the components capable of forming a complex with NLRP3 is PKR [34]. Additionally, oxidative stress is also one of the activators of PKR [39]. It has been assumed that PKR may replace the heat shock protein 90 (Hsp90)/suppressor of G2 allele of skp1 (SGT1) complex, which ensures that the NLR component remains inactive but primed for activation, thus protecting it from degradation [40,41]. Therefore, we speculate about whether PKR can exert multiple functions in CNV. On one hand, PKR activates downstream signal pathways, such as the PI3K/Akt signaling pathway, to upregulate VEGF expression, promoting the progression of CNV. On the other hand, PKR activates the NLRP3 inflammasome to produce mature IL-18, preventing the progression of CNV. This hypothesis will be identified in our future research.

The PI3K/Akt signaling pathway was required for hypoxia-induced expression of hypoxia induced factor 1 (HIF-1) and VEGF in laser-induced rat CNV [15]. The PI3K/Akt/mammalian target of the rapamycin (mTOR) signaling pathway has emerged as an alternative target to inhibit angiogenesis [13,14]. PI3K family members orchestrate innumerable crucial and essential cellular processes, including cell growth, metabolism, survival, and angiogenesis [14,42]. In a mouse CNV model induced by laser photocoagulation, the downregulation of miR-155 attenuates retinal neovascularization via suppressing the PI3K/Akt signaling pathway, indicating that the PI3K/Akt pathway promotes retinal neovascularization [43]. Transmigration assays that are performed while inhibiting PI3K and ras-related C3 botulinum toxin substrate 1 (Rac1) activity result in decreased CEC transmigration [44]. In addition, the CNV-induced increase in the phosphorylation levels of Akt and mTOR is augmented by the downregulation of discoidin domain receptor 2 (DDR2), resulting in aggravated CNV severity [45]. In the present study, the PI3K inhibitor LY294002 greatly decreased the p-PI3K, p-Akt, and VEGF protein levels, but PKR expression was unaffected, indicating that Akt was a downstream molecule of PKR, upregulating VEGF expression.

In conclusion, the present study identified a proangiogenic role for PKR via upregulating the expression of VEGF in the PI3K/Akt signaling pathway in an RF/6A cell chemical hypoxia model and a laser-induced mouse CNV model. These data may suggest PKR as a potential novel target for the prevention and treatment of human AMD. However, further studies should be performed to verify other roles for PKR in CNV and other underlying mechanisms, such as inflammasomes.

## ACKNOWLEDGMENTS

The study was supported by the National Natural Science Foundation of China (81401365), the Natural Science Foundation of the Jiangsu Higher Education Institutions of China (14KJB180018), the Nantong Science and Technology Project (MS12015056, MS12015067), and a project funded by the Priority Academic Program Development of Jiangsu Higher Education Institutions (PAPD). Corresponding authors: chenhuieye@126.com (H. Chen) sangam@ntu.edu.cn (A. Sang)

## REFERENCES

1. Ambati J, Fowler BJ. Mechanisms of age-related macular degeneration. Neuron 2012; 75:26-39. [PMID: 22794258].
2. van Lookeren Campagne M, LeCouter J, Yaspan BL, Ye W. Mechanisms of age-related macular degeneration and

therapeutic opportunities. J Pathol 2014; 232:151-64. [PMID: 24105633].

3. Bhutto I, Lutty G. Understanding age-related macular degeneration (AMD): relationships between the photoreceptor/retinal pigment epithelium/Bruch's membrane/choriocapillaris complex. Mol Aspects Med 2012; 33:295-317. [PMID: 22542780].
4. Solomon SD, Lindsley K, Vedula SS, Krzystolik MG, Hawkins BS. Anti-vascular endothelial growth factor for neovascular age-related macular degeneration. Cochrane Database Syst Rev 2014; 8:CD005139-[PMID: 25170575].
5. Cheung CS, Wong AW, Lui A, Kertes PJ, Devenyi RG, Lam WC. Incidence of endophthalmitis and use of antibiotic prophylaxis after intravitreal injections. Ophthalmology 2012; 119:1609-14. [PMID: 22480743].
6. Carvounis PE, Kopel AC, Benz MS. Retinal pigment epithelium tears following ranibizumab for exudative age-related macular degeneration. Am J Ophthalmol 2007; 143:504-5. [PMID: 17317395].
7. Nagiel A, Freund KB, Spaide RF, Munch IC, Larsen M, Sarraf D. Mechanism of retinal pigment epithelium tear formation following intravitreal anti-vascular endothelial growth factor therapy revealed by spectral-domain optical coherence tomography. Am J Ophthalmol 2013; 156:981-988. [PMID: 23972309].
8. von Holzen U, Pataer A, Raju U, Bocangel D, Vorburger SA, Liu Y, Lu X, Roth JA, Aggarwal BB, Barber GN, Keyomarsi K, Hunt KK, Swisher SG. The double-stranded RNA-activated protein kinase mediates radiation resistance in mouse embryo fibroblasts through nuclear factor kappaB and Akt activation. Clin Cancer Res 2007; 13:6032-9. [PMID: 17947465].
9. Alisi A, Spaziani A, Anticoli S, Ghidinelli M, Balsano C. PKR is a novel functional direct player that coordinates skeletal muscle differentiation via p38MAPK/AKT pathways. Cell Signal 2008; 20:534-42. [PMID: 18164587].
10. Handy I, Patel RC. STAT1 requirement for PKR-induced cell cycle arrest in vascular smooth muscle cells in response to heparin. Gene 2013; 524:15-21. [PMID: 23597922].
11. Harcourt JL, Hagan MK, Offermann MK. Modulation of double-stranded RNA-mediated gene induction by interferon in human umbilical vein endothelial cells. J Interferon Cytokine Res 2000; 20:1007-13. [PMID: 11096458].
12. Imaizumi T, Hatakeyama M, Yamashita K, Ishikawa A, Yoshida H, Satoh K, Taima K, Mori F, Wakabayashi K. Double-stranded RNA induces the synthesis of retinoic acid-inducible gene-I in vascular endothelial cells. Endothelium 2005; 12:133-7. [PMID: 16291516].
13. Zhu Z, Zhong H, Zhou Q, Hu X, Chen D, Wang J, Wu J, Cai J, Zhou S, Chen AF. Inhibition of PKR impairs angiogenesis through a VEGF pathway. Am J Physiol Endocrinol Metab 2015; 308:E518-24. [PMID: 25587101].
14. Follo MY, Manzoli L, Poli A, McCubrey JA, Cocco L. PLC and PI3K/Akt/mTOR signalling in disease and cancer. Adv Biol Regul 2015; 57:10-6. [PMID: 25482988].
15. Yang XM, Wang YS, Zhang J, Li Y, Xu JF, Zhu J, Zhao W, Chu DK, Wiedemann P. Role of PI3K/Akt and MEK/ERK in mediating hypoxia-induced expression of HIF-1alpha and VEGF in laser-induced rat choroidal neovascularization. Invest Ophthalmol Vis Sci 2009; 50:1873-9. [PMID: 19098317].
16. Lou DA, Hu FN. Specific antigen and organelle expression of a long-term rhesus endothelial cell line. In Vitro Cell Dev Biol 1987; 23:75-85. [PMID: 3102454].
17. Wang L, Yang Z, Yu Y, Cui C, Guan H, Chen H. Blockage of tissue factor ameliorates the lesion of laser-induced choroidal neovascularization in mice. Exp Eye Res 2014; 127:117-23. [PMID: 25063201].
18. Balaratnasingam C, Dhrami-Gavazi E, McCann JT, Ghadiali Q, Freund KB. Aflibercept: a review of its use in the treatment of choroidal neovascularization due to age-related macular degeneration. Clin Ophthalmol 2015; 9:2355-71. [PMID: 26719668].
19. Lambert V, Lecomte J, Hansen S, Blacher S, Gonzalez ML, Struman I, Sounni NE, Rozet E, de Tullio P, Foidart JM, Rakic JM, Noel A. Laser-induced choroidal neovascularization model to study age-related macular degeneration in mice. Nat Protoc 2013; 8:2197-211. [PMID: 24136346].
20. Poor SH, Qiu Y, Fassbender ES, Shen S, Woolfenden A, Delpero A, Kim Y, Buchanan N, Gebuhr TC, Hanks SM, Meredith EL, Jaffee BD, Dryja TP. Reliability of the mouse model of choroidal neovascularization induced by laser photocoagulation. Invest Ophthalmol Vis Sci 2014; 55:6525-34. [PMID: 25205860].
21. Gong Y, Li J, Sun Y, Fu Z, Liu CH, Evans L, Tian K, Saba N, Fredrick T, Morss P, Chen J, Smith LE. Optimization of an Image-Guided Laser-Induced Choroidal Neovascularization Model in Mice. PLoS One 2015; 10:e0132643-[PMID: 26161975].
22. Ijima R, Kaneko H, Ye F, Nagasaka Y, Takayama K, Kataoka K, Kachi S, Iwase T, Terasaki H. Interleukin-18 induces retinal pigment epithelium degeneration in mice. Invest Ophthalmol Vis Sci 2014; 55:6673-8. [PMID: 25237159].
23. Takanashi M, Sudo K, Ueda S, Ohno S, Yamada Y, Osakabe Y, Goto H, Matsunaga Y, Ishikawa A, Usui Y, Kuroda M. Novel Types of Small RNA Exhibit Sequence- and Target-dependent Angiogenesis Suppression Without Activation of Toll-like Receptor 3 in an Age-related Macular Degeneration (AMD) Mouse Model. Mol Ther Nucleic Acids 2015; 4:e258-[PMID: 26484944].
24. Veritti D, Sarao V, Lanzetta P. Neovascular age-related macular degeneration. Ophthalmologica 2012; 227:Suppl 111-20. [PMID: 22517121].
25. Haller JA. Current anti-vascular endothelial growth factor dosing regimens: benefits and burden. Ophthalmology 2013; 120:SupplS3-7. [PMID: 23642784].

26. Pindel A, Sadler A. The role of protein kinase R in the interferon response. J Interferon Cytokine Res 2011; 31:59-70. [PMID: 21166592].

27. Garcia MA, Gil J, Ventoso I, Guerra S, Domingo E, Rivas C, Esteban M. Impact of protein kinase PKR in cell biology: from antiviral to antiproliferative action. Microbiol Mol Biol Rev 2006; 70:1032-60. [PMID: 17158706].

28. Williams BR. Signal integration via PKR. Sci STKE 2001; 2001:re2-[PMID: 11752661].

29. Marchal JA, Lopez GJ, Peran M, Comino A, Delgado JR, Garcia-Garcia JA, Conde V, Aranda FM, Rivas C, Esteban M, Garcia MA. The impact of PKR activation: from neurodegeneration to cancer. FASEB J 2014; 28:1965-74. [PMID: 24522206].

30. Morel M, Couturier J, Lafay-Chebassier C, Paccalin M, Page G. PKR, the double stranded RNA-dependent protein kinase as a critical target in Alzheimer's disease. J Cell Mol Med 2009; 13:8A1476-88. [PMID: 19602051].

31. Marques JT, White CL, Peters GA, Williams BR, Sen GC. The role of PACT in mediating gene induction, PKR activation, and apoptosis in response to diverse stimuli. J Interferon Cytokine Res 2008; 28:469-76. [PMID: 18729737].

32. Singh M, Patel RC. Increased interaction between PACT molecules in response to stress signals is required for PKR activation. J Cell Biochem 2012; 113:2754-64. [PMID: 22473766].

33. Geisen P, McColm JR, Hartnett ME. Choroidal endothelial cells transmigrate across the retinal pigment epithelium but do not proliferate in response to soluble vascular endothelial growth factor. Exp Eye Res 2006; 82:608-19. [PMID: 16259980].

34. Lu B, Nakamura T, Inouye K, Li J, Tang Y, Lundback P, Valdes-Ferrer SI, Olofsson PS, Kalb T, Roth J, Zou Y, Erlandsson-Harris H, Yang H, Ting JP, Wang H, Andersson U, Antoine DJ, Chavan SS, Hotamisligil GS, Tracey KJ. Novel role of PKR in inflammasome activation and HMGB1 release. Nature 2012; 488:670-4. [PMID: 22801494].

35. Doyle SL, Ozaki E, Brennan K, Humphries MM, Mulfaul K, Keaney J, Kenna PF, Maminishkis A, Kiang AS, Saunders SP, Hams E, Lavelle EC, Gardiner C, Fallon PG, Adamson P, Humphries P, Campbell M. IL-18 attenuates experimental choroidal neovascularization as a potential therapy for wet age-related macular degeneration. Sci Transl Med 2014; 6:230ra44-[PMID: 24695684].

36. Franchi L, Munoz-Planillo R, Nunez G. Sensing and reacting to microbes through the inflammasomes. Nat Immunol 2012; 13:325-32. [PMID: 22430785].

37. Doyle SL, Campbell M, Ozaki E, Salomon RG, Mori A, Kenna PF, Farrar GJ, Kiang AS, Humphries MM, Lavelle EC, O'Neill LA, Hollyfield JG, Humphries P. NLRP3 has a protective role in age-related macular degeneration through the induction of IL-18 by drusen components. Nat Med 2012; 18:791-8. [PMID: 22484808].

38. Kauppinen A, Niskanen H, Suuronen T, Kinnunen K, Salminen A, Kaarniranta K. Oxidative stress activates NLRP3 inflammasomes in ARPE-19 cells–implications for age-related macular degeneration (AMD). Immunol Lett 2012; 147:29-33. [PMID: 22698681].

39. Pyo CW, Lee SH, Choi SY. Oxidative stress induces PKR-dependent apoptosis via IFN-gamma activation signaling in Jurkat T cells. Biochem Biophys Res Commun 2008; 377:1001-6. [PMID: 18976633].

40. Martinon F, Mayor A, Tschopp J. The inflammasomes: guardians of the body. Annu Rev Immunol 2009; 27:229-65. [PMID: 19302040].

41. Mayor A, Martinon F, De Smedt T, Petrilli V, Tschopp J. A crucial function of SGT1 and HSP90 in inflammasome activity links mammalian and plant innate immune responses. Nat Immunol 2007; 8:497-503. [PMID: 17435760].

42. Marone R, Cmiljanovic V, Giese B, Wymann MP. Targeting phosphoinositide 3-kinase: moving towards therapy. Biochim Biophys Acta 2008; 1784:159-85. [PMID: 17997386].

43. Zhuang Z. Xiao q, Hu H, Tian SY, Lu ZJ, Zhang TZ, Bai YL. Down-regulation of microRNA-155 attenuates retinal neovascularization via the PI3K/Akt pathway. Mol Vis 2015; 21:1173-84. [PMID: 26539029].

44. Peterson LJ, Wittchen ES, Geisen P, Burridge K, Hartnett ME. Heterotypic RPE-choroidal endothelial cell contact increases choroidal endothelial cell transmigration via PI 3-kinase and Rac1. Exp Eye Res 2007; 84:737-44. [PMID: 17292356].

45. Zhu T, Zhu J, Bu X, Zhao H, Zhang S, Chang Y, Li R, Yao L, Wang Y, Su J. The anti-angiogenic role of discoidin domain receptor 2 (DDR2) in laser-induced choroidal neovascularization. J Mol Med (Berl) 2015; 93:187-98. [PMID: 25355563].


Articles are provided courtesy of Emory University and the Zhongshan Ophthalmic Center, Sun Yat-sen University, P.R. China. The print version of this article was created on 2 December 2016. This reflects all typographical corrections and errata to the article through that date. Details of any changes may be found in the online version of the article.